International Journal of Applied Science and Engineering
2009. 6, 3: 229-237

Partial Discharge Precise Source Location Using Acoustic Emission Method for a Waveguide Functional High-Voltage Cast-Resin Dry-Type Transformer

Ching-Chau Su[a*], Cheng-Chi Tai[b], Chien-Yi Chen[a], Ju-Chu Hsieh[a]

[a] *Ph.D. students, Department of Electrical Engineering, National Cheng Kung University.*
[b] *Professor, Department of Electrical Engineering, National Cheng Kung University.*

Abstract: This study adopts the acoustic emission (AE) method to measure partial discharges (PD) in a cast-resin dry-type transformer and proposes a waveguide atop the high-voltage winding of the transformer to improve the propagation of the PD acoustic signals occurring in said winding to acoustic emission sensors used. A waveguide is proposed by us to mend the signals' quick attenuation amid the winding's coils and to eliminate the discharge, encountered by the present methods, from the winding to the sensor. We also study how to analyze the AE signals and how to locate a PD's source, down to the coil level. Finally, a waveguide is actually installed on a real cast-resin dry-type transformer; the measurements and the locating of PDs' AE signals for said transformer are carried out. This proposed waveguide forms a new acoustic-wave propagation route to resolve the acoustic-wave propagation difficulty and, meanwhile, eliminate the high-voltage winding's discharge danger to the sensor. This study demonstrates a feasible new simple, safe and economical solution for diagnosing and locating PDs in the transformer.

Keywords: Partial discharges (PD); Acoustic emission; Cast-resin dry-type transformer; Waveguide.

1. Introduction

High-tech factories often use cast-resin dry-type transformers instead of oil-immersed transformers, for the latter could cause a fire when at fault or during failure. Cast-resin dry-type transformers hold some merits including moisture-resistance, anti-flame quality, low noise and public hazard-free characteristics and, hence, are often adopted in places such as the high-tech industry, the aviation industry, hospitals and the like. To raise the power transmission efficiency, electric power companies usually step up the voltage, forcing the transformers' insulation materials to bear an even greater electric stress; in case the insulation performance deteriorates, a PD will follow. If a correct diagnosis cannot be furnished at this time, the insulation resin in the high-voltage winding of a cast-resin dry-type transformer will break down, bringing the production line to a halt and, consequentially, causing unneeded financial losses.

Up to date, the PD measurement methods for cast-resin dry-type transformers are divided into two categories, namely the electric and the non-electric methods.

With an acoustic measurement method, it is easy to locate a discharge source [1] using an ultrasonic microphone, but in case the PD

* Corresponding author; e-mail: ea006@mail.njtc.edu.tw *Accepted for Publication: April 03, 2009*

sources are hidden inside the facilities and blocked by dielectrics segregated from the air, e.g. an insulation oil, resin, SF_6, etc., the discharge's acoustic signal will not be easy to propagate to the outside. Hence, we adopt an acoustic emission sensor to measure the internal PDs.

When an internal PD occurs, it will form an acoustic source and emit an acoustic wave, *i.e.* a mechanical elastic wave, which will propagate around the inside of the facility, as shown in Figure 1. Such internal acoustic wave inside the facility is hard to measure by a non-contact ultrasonic microphone.

We fasten the AE sensor to the facility's surface and utilize the piezoelectric material inside the sensor to convert the mechanical elastic wave into an electric signal; the AE signal is then extracted using a pre-amplifier and a filter. The AE measurement method adopted can acquire acoustic signals with a frequency scattering between 30 k to 200 kHz [2]; in comparison with other methods, the frequency needed to be processed by this method is the lowest; hence, using this method will require the lowest cost for signal processing, a great advantage over other methods.

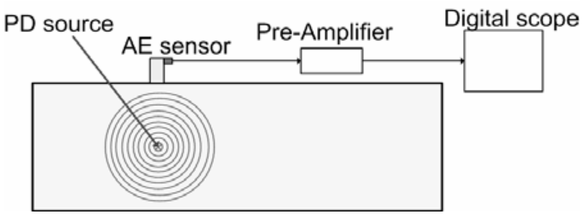

Figure 1. The propagation of the acoustic wave.

2. System and components

(a) The cast-resin dry-type transformer

As shown in Figure 2, a high-voltage-coil set of the cast resin transformer comprises an iron core formed by a plurality of stacked silicon steel sheets and wound with wires to form three high-voltage coils. The three high-voltage coils are embedded with insulated resin to form the high-voltage-coil set of the cast resin transformer. Each of the high-voltage coils is primarily constructed by wound wires which are embedded with insulated material to form an annular coil. The high-voltage coil further comprises a high-voltage connector which is composed of terminals and high-voltage contacts. Heat-dissipation is achieved by air convection in the high-voltage coil. Compared with the traditional oil-immersed transformer, the cast resin transformer needs no oil and is safer without flaming. In addition, the cast resin transformer exhibits merits of moisture-proof, less noise and flame-retardant, and thus is suitable for application in hospitals, high-tech plants, rapid transit system, high speed rail and airport.

(b) The high-voltage winding of the cast-resin dry-type transformer

The production method for the high-voltage winding involves a layer-by-layer winding of foil-type aluminum coils, as shown in Figures. 3 and 4.

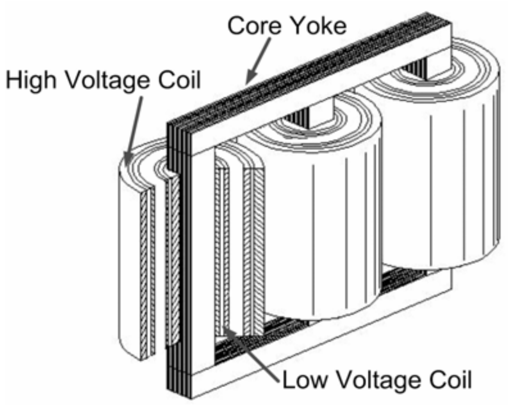

Figure 2. The structure of a cast-resin dry-type transformer.

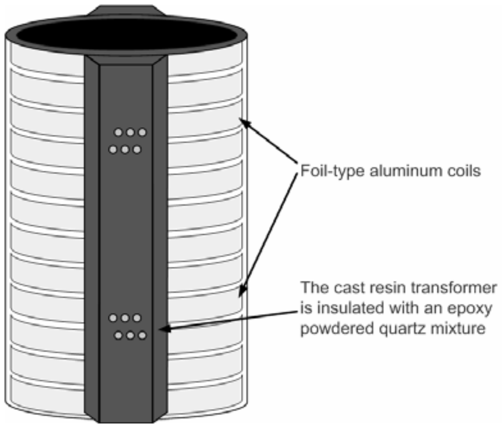

Figure 3. The structure of the high-voltage winding.

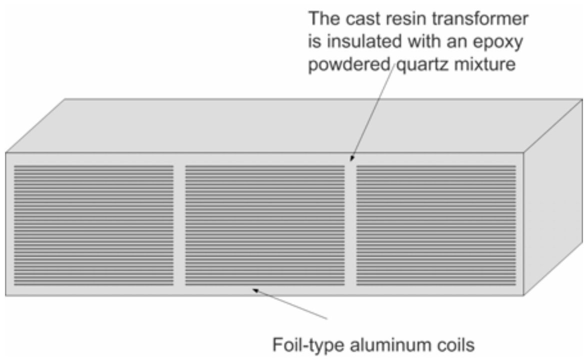

Figure 4. The cross section of the high-voltage winding.

3. Experiments

3.1. Acoustic sensor selection

(a) Using the pencil lead break to emulate a PD's AE signal source

According to ASTM E976-00 [3], a 2H pencil lead of 0.3 mm (or 0.5 mm) in diameter shall be broken on the surface of the high-voltage winding with a distance of 10 cm from the AE sensor. When the pencil lead break is made, an instantaneous stress will be generated on the contact point between the tip and the high-voltage winding so as to form an acoustic impulse signal on the high-voltage winding, the elastic wave of which will propagate toward all directions, as shown in Figure 5. With this acoustic impulse signal, we can simulate an occurring PD due to insulation deterioration or the like.

We observe from the high-voltage winding's horizontal cross-section diagram shown in Figure 6 that the resin wall is the thickest at the two connection-lead sides; while in the middle portion, the resin wall is the thinnest, only 2-mm thick. This material's thickness is far smaller than the wavelength; therefore, when an AE signal, be it a longitudinal wave or a transversal wave, propagates to this area, only a plate wave will be left to the resin. From Figure 7 we observe that the wide-band-type sensor and the pre-amplifier are prone to ambient acoustic interferences; hence, we need to select an ultrasonic range to operate. Besides, the frequency response under 300 kHz for the wideband-type sensors is not acceptable; hence, we shall select a low-frequency type (MODEL VS30-V), or a low-frequency resonant-type (MODEL VS150-M), sensor and match it up with a narrow-band pre-amplifier (MODEL AEP3:30 kHz ~ 300 kHz, 34 dB).

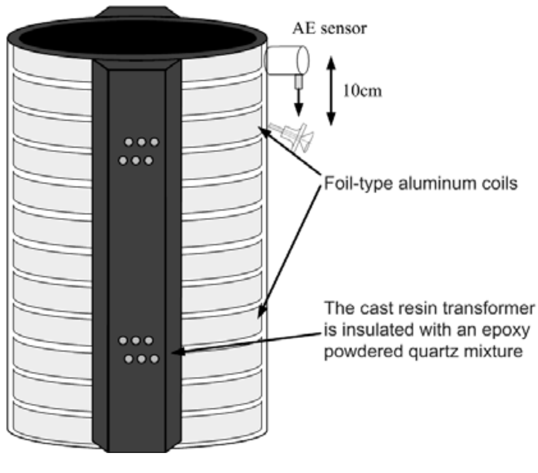

Figure 5. Using the pencil lead break to emulate a PD's AE signal.

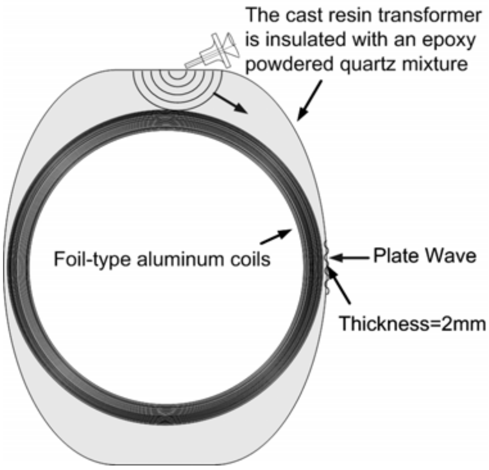

Figure 6. The high-voltage winding's horizontal cross-section diagram.

(b) The spectrum analysis of AE signals

The piezoelectric material inside the AE sensor can convert the elastic wave propagating inside the high-voltage winding into an electric signal. The emulation of a PD due to insulation deterioration, such as by making a pencil leak break on the winding's surface, is shown in Figure 5. To determine an optimal bandwidth for the AE sensor and the filter, we look into the frequency-spectrum characteristics of the AE signals propagating inside the high-voltage winding for various AE sensors and pre-amplifiers with different frequency response.

Using a wideband pre-amplifier (Model AEP4, 2 kHz to 3.8 MHz, 40 dB) along with a wideband AE sensor (Model AE2045S), an AE signal obtained as shown in Figure 7(a). Its frequency spectrum is shown in Figure 7(b). The main frequency of the AE signal scatters between 5 kHz to 200 kHz, and from the time-domain signal, we can clearly observe the characteristics of the Lamb wave and the plate wave, either in the extensional or in the flexural mode[1][4]. Since the signal source is out-of-plane, its flexural mode possesses a greater magnitude. But the signal's frequency is only at 5 kHz approximately; hence, the signal is not suitable for PD recognition in the experiment, for it is prone to the interferences of the core's vibration and other ambient acoustic noises.

The AE signal and its frequency spectrum analysis obtained by using the AEP3 narrow-band pre-amplifier with the resonant type AE sensor (Model VS150-M) and the low-frequency AE sensor (Model VS30-V) are shown in Figure 8. We observe from Figure 8 that the main frequencies of the AE signal scatter between 30 kHz to 160 kHz; but the resonant type sensor is prone to cause us misjudge the real frequency's location as there is no maximum-power signal at 150 kHz; thus, the real frequency must lie at an even lower frequency. There exists a fairly flat frequency-response characteristic between 23 kHz to 80 kHz for the low-frequency AE sensor (Model VS30-V); we observe that the actual PD's AE-signal frequency lies adjacent to 50 kHz. Comparing Figure 8(a) with 8(b), we detect that the acoustic-waveform amplitude of VS30-V is four-fold as much as that of VS150-M. Since selecting lower-frequency signals can reduce the cost of post-stage signal processing, VS30-V, hence, is more suitable than VS150-M for PD signal measurements.

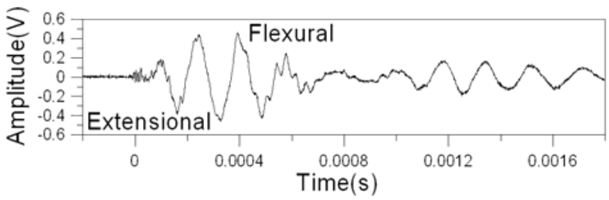

(a)

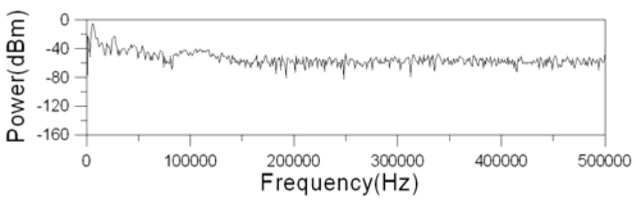

(b)

Figure 7. (a) A typical AE signal measured by the wideband AE2045S pre-amplifier along with a wideband sensor, and (b) the signal's frequency spectrum.

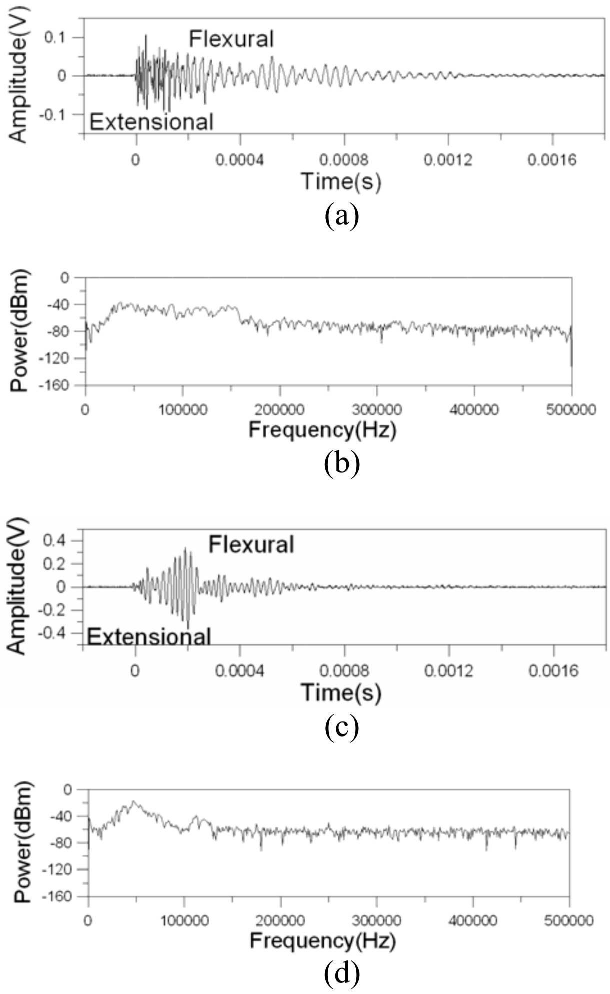

Figure 8. The AE signal and its freque ncy-spectrum analysis of the narrow-band pre-amplifier and the low-frequency type sensor (a) VS150-M's AE-signal waveform; (b) VS150-M's AE-signal frequency response; (c) VS30-V's AE-signal waveform; (d) VS30-V's AE-signal frequency response.

3.2. Design scheme

(a) The installation method for the AE sensor

Directly installing an AE sensor on the high-voltage winding will set off the high-voltage winding's discharge phenomenon toward the sensor, as shown in Figure 9. As the metal shell of the AE sensor is connected to the ground terminal of the measurement system, the AE sensor installed on the high-voltage winding will change the winding's electric-field distribution; the field's intensity will be the strongest for the sensor near the high-voltage winding, as shown in Figure 10. The insulation of the air adjacent to the sensor's base will be broken up for being unable to bear such high intensity, resulting in the discharge from the high-voltage winding toward the AE sensor. We propose that a waveguide is to be installed atop the surface of the high-voltage winding to prevent the sensor from affecting the electric-field distribution on the winding's surface after said sensor's installation.

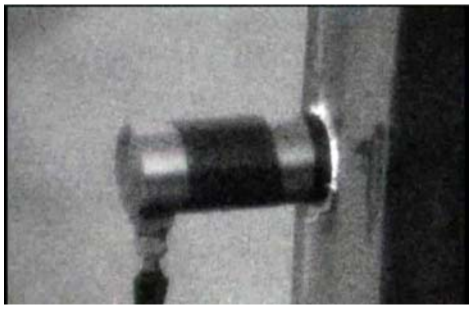

Figure 9. The discharge phenomenon from the high-voltage winding toward the AE sensor.

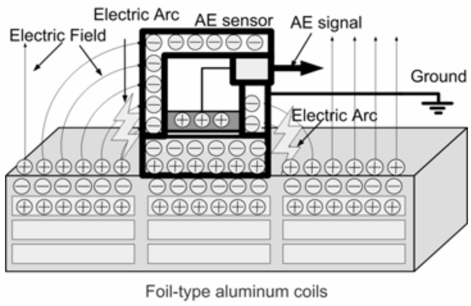

Figure 10. The high-voltage winding's electric-field distribution altered by the AE sensor.

(b) The design of a waveguide

The purpose for a waveguide designed atop the high-voltage winding is to provide a good channel for the acoustic-wave propagation to guide out a PD's AE signal. From the viewpoint of measurement, a good waveguide to a high-voltage winding must: first, render a very good acoustic-wave propagation route; second, not change the winding's electric-field distribution to avoid changing the winding's original insulation strength designed, and third, not have a measurement sensor adhering to the winding's surface.

First, the waveguide's propagation speed and attenuation coefficient must all be close to that of metal; a tempered glass not only conforms with this requirement but also has a great advantage on its cost and procurement. Second, the waveguide's material must be of high insulation strength quality; a tempered glass's insulation strength is rather high. Third, the AE sensor must maintain a safe distance with the high-voltage winding to prevent the winding from discharging toward the sensor. We hence install the sensor between the top and bottom bars of the transformer's clamping frame, as shown in Figure 11.

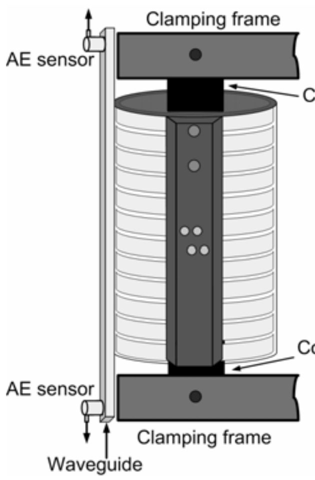

Figure 11. The design of the waveguide and the installation method of the AE sensor.

(c) Using the waveguide to improve the acoustic-wave propagation

This study adopts two pairs of AE sensors to analyze the AE signal's attenuation, as shown in Figure 12 [5], where the first pair of sensors, AE2 and AE3, is installed on the high-voltage winding and the second pair, AE1 and AE4, on the waveguide. Next, the pencil lead break is made at locations P1 and P2, respectively. The acoustic-wave amplitude is the maximum amplitude of AE signal so we can measure two sets of acoustic-wave amplitude ratio tabulated in Table 1. When the pencil lead breaks is made at a distance of 60 cm away from P0, the acoustic-wave amplitude ratio in the waveguide (AE4/AE1) is 39.3%, comparing to the acoustic-wave amplitude ratio of 5.1% measured from the high-voltage winding (AE3/AE2). Comparing, again, the amplitude of AE4 with that of AE3, the AE4's amplitude on the waveguide is 40.7 mV, and the amplitude of AE3 on the high-voltage winding is only 3.98 mV, which is rather minute, closing to the limit of the AE sensor's sensitivity. Next, the pencil lead break is shifted from P2 to P1, and the acoustic-wave amplitude ratio measured twice with AE4 is 48.4%, while with AE3 only 29%. The above test result verifies that the proposed waveguide indeed can improve the acoustic-wave propagation on the high-voltage winding. The AE signals of AE1 and AE4 are shown in Figure 13. The acoustic-wave's arriving-at-sensor-time difference for the two sensors, T, is 117.21 μs; since the distance between the two sensors is 40 cm, the acoustic-wave speed in the waveguide can be computed and arrives at 3,413 m/s.

(d) Measurement process

We first install the waveguide atop the high-voltage winding, and then install two VS30-V AE sensors on the waveguide, with a pre-amplifier of 49 dB. The actual measurement system's block diagram is shown in Figure 14.

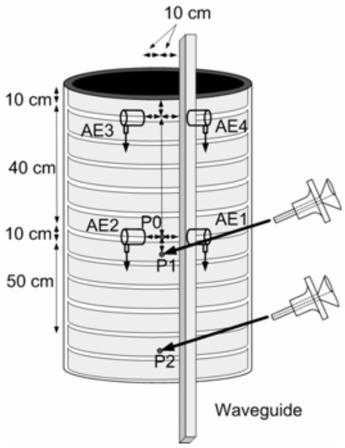

Figure 12. The acoustic wave test in the waveguide.

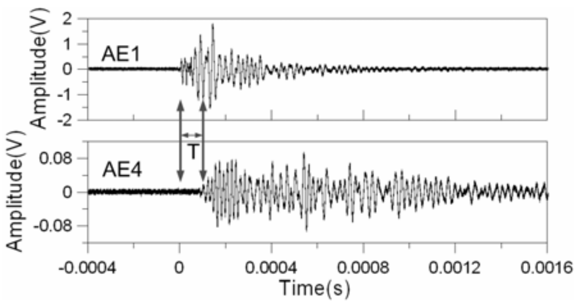

Figure. 13. AE signals of AE1 and AE4 sensors.

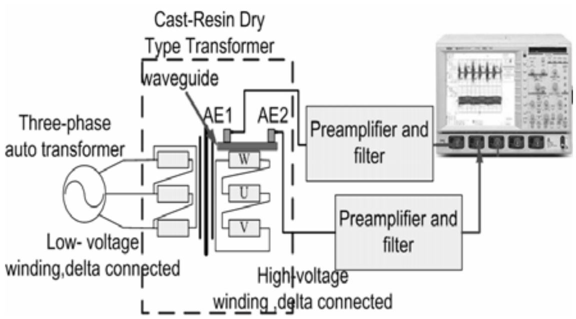

Figure 14. The actual measurement system's block diagram.

Table 1. The two pairs' acoustic-wave amplitude comparison.

	Acoustic-wave amplitude comparison on the waveguide			Acoustic-wave amplitude comparison on the high-voltage winding		
Pencil-lead -break location	AE1	AE4	Ratio (AE4 / AE1)	AE2	AE3	Ratio (AE3 / AE2)
P1 60 cm	1.48 V	84 mV	5.6%	> 2.8 V	13.7 mV	< 0.4%
P2 100 cm	102 mV	40.7 mV	39.3%	77 mV	3.98 mV	5.1%
Ratio (P2/P1)	6.89 %	48.4%		< 2.74%	29%	

(e) Locating of a PD

The greatest advantage of the AE method lies in locating a PD. Only with the AE method can we diagnose which winding package is discharging or even locate which coil in the high-voltage winding is discharging, as shown in Figure 15. Assuming that the PD's location is away from the center of the waveguide by x and that the distance between the two sensors is L, the acoustic wave, once propagating in the waveguide, will be away from AE1 by ($L/2 + x$), and from AE2 by ($L/2 - x$). If the acoustic-wave's arriving-at-sensor-time difference for the two sensors is T and since the propagation-distance difference is $2x$, we, hence, can obtain that $x = (3413*T/2)$ m, using an acoustic-wave velocity of 3413 m/s in the waveguide. We can thus calculate the distance between the PD source and the center of the waveguide, x; the PD's coil location thus can be calculated, too.

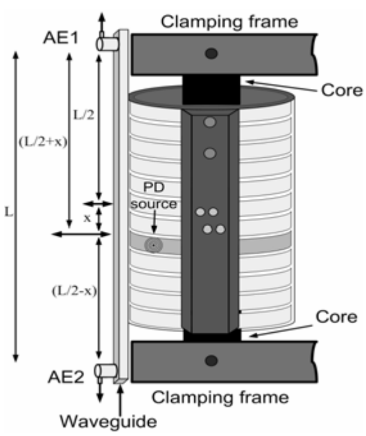

Figure 15. Locating a PD.

(f) The actual PD-measurement AE signals

The three-phase autotransformer is adjusted to 130 V. The PD's AE signals measured are shown in Figure 16, where the signal arriving-at-sensor-time difference for the two sensors, T, is equal to 64.6 μs. From the acoustic wave test shown in Figure 12, we can calculate and obtain the acoustic-wave velocity in the waveguide as 3413 m; finally, we can calculate and attain that the distance between the coil of the PD source and the center of the waveguide is 11 cm.

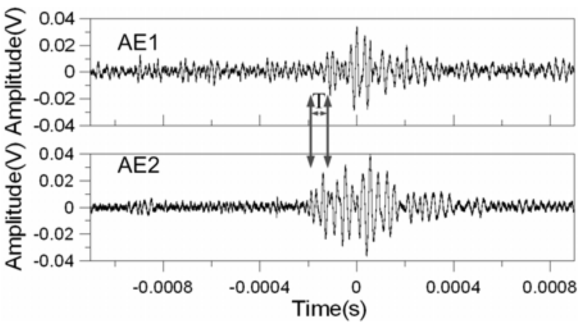

Figure 16. The AE signals generated by the PDs.

4. Discussion

The advantages of the AE method applied to measuring a cast-resin dry-type transformer's PDs are: (1) This method can be used to locate which high-voltage winding has a PD source; furthermore, using the above-mentioned source location method, we can pinpoint the particular coil's location where the PD occurs. (2) There exist much less false alarms, which are frequently encountered by the electric method due to oversensitivity problem. (3) Since this is related to acoustic signal processing, the cost for the latter-stage computer's signal processing is rather low.

The major problems related to the implementation of the AE method are: (1) Fiber glass will be added in the resin during the manufacturing process of the high-voltage winding. The fiber glass, however, holds an apparent absorption effect toward acoustic waves, resulting in a severe attenuation to the propagating acoustic-wave signals inside the high-voltage winding. (2) The installation of the AE sensor right on the high-voltage winding surface will set off the winding's discharge phenomenon toward the AE sensor.

5. Conclusions

The proposed waveguide forms a new acoustic-wave propagation route to resolve the acoustic-wave propagation problem and, meanwhile, eliminate the high-voltage winding's discharge danger to the sensor. This study renders a new safe, feasible and economical solution, with simplicity, for diagnosing and locating the PDs.

6. Acknowledgements

This research was supported by the grant from National Science Council, Taiwan, ROC (NSC 93-2622-E-006-002). Also, this work made use of Shared Facilities supported by the Program of Top 100 Universities Advancement, Ministry of Education, Taiwan.

7. References

[1] Lundgaard, L. E. 1992. "*Partial Discharge – Part XIV Acoustic Partial Discharge Detection - Practical Application*," Electrical Insulation Magazine, IEEE, Volume 8, No. 5: 34-43.

[2] IEEE Trial-Use Guide for the Detection of Acoustic Emissions from Partial Discharges in Oil-Immersed Power Transformers, IEEE Std C57. 127-2000.

[3] Standard Guide for Determining the Reproducibility of Acoustic Emission Sensor Response, ASTM Standard E976-00.

[4] Prosser, W. H., Gorman, M. R.1993. "*Plate Mode Velocities in Graphite/Epoxy Plates* ", the *Journal of the Acoustical Society of America*, 10

[5] Chen, J. F., Tai, C. C., Liang, T. J., Su, C.

C., Yi, C. S., Chen C. Y. 2008. "*High-voltage transformer coil with acoustic wave guiding function*", U. S. Patent 7 339 447, Mar. 4.